Simple Harmonic Motion within a Torsional Oscillator

The Ohio State University, Department of Physics, Columbus, OH 43210

Colin Voorhis
Partners: Emily Macbeth, Hirak Basu

April 24th, 2025

Abstract

This experiment analyzes the behavior of a torsional oscillator, a mechanical system which undergoes a periodic rotation around a set equilibrium. A rotor is displaced by a small rotational angle and released to generate simple harmonic motion. This rotor is then subjected to several damping regimes with varying dependence on the angular velocity of the rotor. The displacement of this rotor is recorded using an angular transducer and fitted to extract the angular frequency of several oscillations. The rotor's moment of inertia is measured as $I_0 = 6.65 \pm 0.046 \cdot 10^{-4}\,\mathrm{kg/m^2}$ and its torsional constant is measured as $\kappa = 4.439 \pm 0.02 \cdot 10^{-2}\,\mathrm{N\,m}$.

1 Introduction

Simple harmonic motion is a physical phenomenon where a system is drawn to an equilibrium by a force proportional to its displacement from equilibrium. This concept is used to model the behavior of many systems, including springs, pendulums, electromagnetic waves, and vibrations. This experiment analyzes torsional oscillations, rotations which in this case can be modeled by simple harmonic motion. The oscillator is also placed under several damping regimes where the restorative force on the rotor is reduced at a constant rate or proportional to the angular velocity of the oscillator.

2 Theory

2.1 Static Oscillator

In this experiment, a torsional oscillator experiences $\vec{\tau}$ with magnitude proportional to its angular displacement θ. The two are related via a torsion proportionality constant κ:

$$\tau = -\kappa\theta \tag{1}$$

This τ is generated by two masses which are hung along pulleys attached to the shaft of the oscillator. In this case the magnitude of τ is

$$\tau = 2mrg \tag{2}$$

where:

- m is the mass of one hung mass
- r is the radius of the rotor shaft
- g is acceleration due to gravity

The oscillator outputs a voltage which is linearly proportional to the angular position of the rotor for small displacements. See Appendix A.1 for further information.

2.2 Undamped Oscillator

The behavior of a torsional oscillator can be modeled using a one-dimensional differential equation:

$$\ddot{\theta} = -\frac{\kappa}{I}\theta \tag{3}$$

where:

- $\ddot{\theta}$ is the angular acceleration of the oscillator
- θ is the angular displacement of the oscillator
- κ is the torsional constant of the oscillator
- I is the scaler moment of inertia of the oscillator

See Appendix A.2 for a derivation of this equation. One solution to this differential equation is as follows:

$$\theta(t) = A\sin(\omega t + \phi_0) \tag{4}$$

where:

- A is the amplitude of the motion
- ω is the angular frequency of oscillation
- ϕ_0 is a phase constant

For small values of θ the motion of this oscillator can be treated as simple harmonic motion. In this case the oscillation has a period T defined as

$$T = 2\pi\sqrt{\frac{\boldsymbol{I}}{\kappa}} \tag{5}$$

and corresponding angular frequency

$$\omega = \frac{2\pi}{T} = \sqrt{\frac{\kappa}{\boldsymbol{I}}} = \sqrt{\frac{\kappa}{\boldsymbol{I_0} + n\boldsymbol{I_q}}} \tag{6}$$

where:

- $\boldsymbol{I_0}$ is the moment of inertial of the rotor
- $\boldsymbol{I_q}$ is the moment of inertia of a pair of brass quadrants
- n is the number of quadrant pairs on the rotor

This equation can be rearranged to give

$$\omega^{-2} = \frac{n\boldsymbol{I_q}}{\kappa} + \frac{\boldsymbol{I_0}}{\kappa} \tag{7}$$

This equation can be fitted to extract the parameters κ and $\boldsymbol{I_0}$.

2.3 Linear Damping

Linear damping can be applied to the torsional oscillator using magnetic breaks. Here the damping force F_d relies linearly on the velocity v of the system and a damping constant b_1:

$$F_d = -b_1 v \tag{8}$$

This motion is described by the following differential equation:

$$\ddot{\theta} = -\frac{\kappa}{I}\theta + \frac{b_1}{I}\dot{\theta} \tag{9}$$

There are three different types of damped behavior that this system can exhibit depending on the magnitude of b_1. We define a natural undamped frequency $\omega_0 = \sqrt{\kappa/I}$ and damping coefficient $\gamma = b_1/2I$ to categorize these different behaviors:

- Underdamped ($\gamma^2 < \omega_0^2$): The oscillator will exhibit sinusoidal oscillations within a decaying exponential envelope, eventually returning to its equilibrium position.
- Critically Damped ($\gamma^2 = \omega_0^2$): The oscillator will return to its equilibrium position without oscillating as efficiently as possible.
- Overdamped ($\gamma^2 > \omega_0^2$): The oscillator will return to its equilibrium position without oscillating, but over a longer timescale than the critically damped case.

The solution to Eq. 9 will vary depending on if the oscillator is underdamped, critically damped, or overdamped.

One solution for the underdamped oscillator is to treat the system as oscillating within an "envelope" that bounds its amplitude. The system will still oscillate as described in Eq. 4, but within an overarching decaying exponential: [1]

$$\theta(t) = Ae^{-Bt}\cos(Ct - D) + E \tag{10}$$

where A, B, C, D, and E are fitting parameters. A is dependent on the oscillation's initial amplitude, D is dependent on it's initial phase, E is it's equilibrium displacement, and $B = \gamma$. C depends on γ and ω_0: [1]

$$C = \sqrt{\omega_0^2 - \gamma^2} \tag{11}$$

A critically damped oscillator can be modeled as a single decaying exponential function, with no envelope:

$$\theta(t) = Ae^{-Bt} + C \tag{12}$$

An overdamped oscillator can be modeled as a sum of multiple decaying exponential functions:

$$\theta(t) = Ae^{Ct} + Be^{Dt} \tag{13}$$

where A, B, C, and D are fitting parameters. In this case, C and D are related to ω_0:

$$\begin{aligned} C &= -\gamma + \sqrt{\gamma^2 - \omega_0^2} \\ D &= -\gamma - \sqrt{\gamma^2 - \omega_0^2} \end{aligned} \tag{14}$$

2.4 Constant Damping

Constant damping can be applied to the torsional oscillator using sliding friction between tensioned strings and the rotor shaft. Here the damping force's magnitude is constant and its direction is always opposite that of the velocity:

$$F_d = -b_0 \frac{v}{|v|} \tag{15}$$

This motion is described by the following differential equation:

$$\ddot{\theta} = -\frac{\kappa}{I}\theta + \frac{b_0}{I} \tag{16}$$

In this case, $\theta(t)$ can also be modeled as an oscillation within an envelope. In this case, the envelope is a linear function; the damping force is constant, and so will reduce the amplitude of the oscillation system linearly over time:

$$\theta(t) = A \cdot (mt + b) \cdot \cos(\omega_0 t + \phi) + y \tag{17}$$

In this equation:

- A is a fitting parameter related to the initial amplitude of the oscillation
- m is the slope of the linear envelope
- b is the y-intercept of the linear envelope
- ω_0 is the natural angular frequency of the oscillation
- ϕ is the phase constant of the oscillation
- y is the equilibrium position of the oscillation

3 Methods

The following section is based on the TeachSpin Torsional Oscillator manual [1].

The torsional oscillation in this experiment is generated using a steel torsion wire attached to a rotor shaft, disk, and a set of permanent magnets. The system's moment of inertia can be increased by setting brass quadrants into slots on the rotor disk. The rotor can be angularly displaced by using the apparatus's Helmholtz coils to generate a magnetic field across the rotor's magnets. The angular displacement of the rotor can be recorded by eye or via an angular position transducer, which outputs a voltage proportional to the angular displacement of the rotor. See Appendix A.1 for further information on this conversion.

A constant torque can be applied to the rotor using a pulley system. Strings are attached to the rotor shaft, run through a pulley, and used to hold masses on each side of the rotor. Eq. 2 gives the torque applied by these masses.

The measurements in this lab all have uncertainties derived from the limited precision of angular displacement and voltage measurements. See Appendix A.1 for further information.

3.1 Damping

Linear damping can be applied using magnetic breaks which induce eddy currents in the copper rotor disk. These eddy currents generate a magnetic field that oppose the motion of the rotor. The magnitude of this opposing field is proportional to the velocity of the rotor. The strength of this damping can also be increased by reducing the distance between the breaks and disk. [1]

Constant damping can be applied using two strings put in tension against the rotor shaft. The friction between the strings and shaft generates a damping force independent of the rotor's velocity. The strength of this damping can be increased by increasing the tension on the strings. This increases the normal force the rotor applies to the strings, which in turn increases the magnitude of the friction force between them. [1]

4 Data Analysis and Results

Figure 1 plots angular position against applied torque for the static oscillator. Torque was calculated using Eq. 2, and the data was fit to Eq. 1. This fit measured the torsional constant of the system as $\kappa = 4.439 \pm 0.02 \cdot 10^{-2}\,\mathrm{N\,m}$ with $\chi^2/\mathrm{dof} = 2.25$.

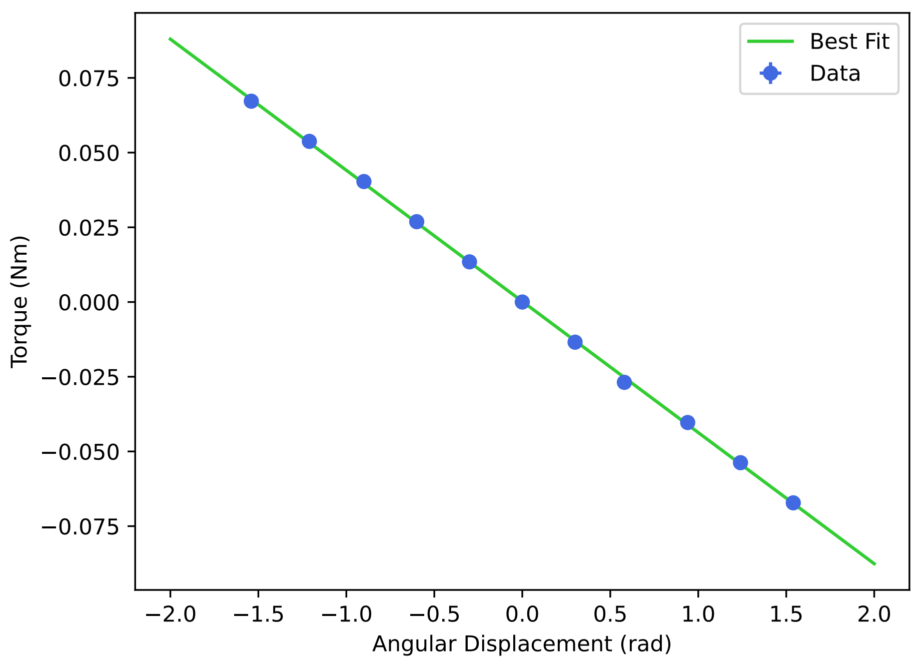

Figure 1: This plot displays the angular displacement of an undamped oscillator as a function of applied torque. The resulting fit has $\chi^2/\mathrm{dof} = 2.25$. Error bars are present, but small, for both axes.

Figure 2 plots one sample of angular position against time for an undamped oscillator. 15 samples were taken with a variable number of brass quadrants and starting amplitudes. Note that each brass quadrant has a moment of inertia of $I_q = 1.842 \pm 0.126 \cdot 10^{-4}\,\mathrm{kg\,m^2}$. See Appendix A.3 for a derivation of this value. Each data sample was fitted to Eq. 4, the results of which are summarized in Table 1. The results indicate agreement with the model proposed in Eq. 6, where ω decreases with increasing I, and is independent of amplitude. A $\chi^2/\mathrm{dof} > 1$ indicates errors for these samples are underestimated.

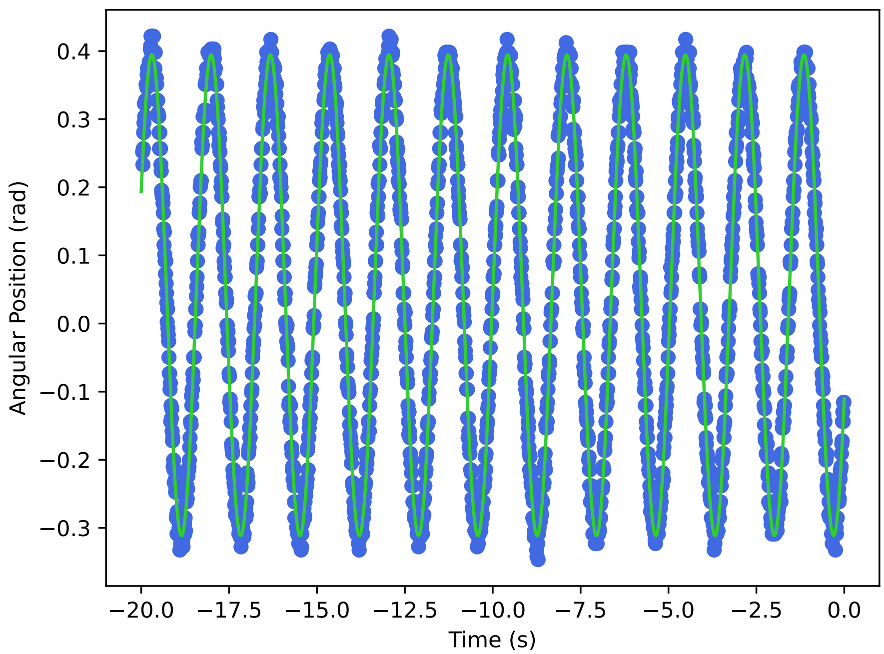

Figure 2: This plot displays the angular displacement of an undamped oscillator as a function of time. This sample has 4 brass quadrants with a starting amplitude of 0.9 rad. The resulting fit has $\chi^2/\mathrm{dof} = 53.3$. Error bars are not included, as they obscure the data and fit when included.

Number of Quadrant Pairs	Amplitude (rad)	Angular Frequency (rad)	χ^2/dof
	0.4	5.415 ± 0.004	336.1
0	0.9	5.412 ± 0.002	56.1
	1.4	5.411 ± 0.001	27.0
	0.4	4.801 ± 0.003	324.0
1	0.9	4.796 ± 0.001	53.3
	1.4	4.791 ± 0.001	20.9
	0.4	4.346 ± 0.003	368.6
2	0.9	4.340 ± 0.001	71.7
	1.4	4.340 ± 0.001	27.9
	0.4	4.003 ± 0.003	381.9
3	0.9	3.991 ± 0.002	94.8
	1.4	3.993 ± 0.001	40.8
	0.4	3.725 ± 0.003	493.2
4	0.9	3.717 ± 0.001	80.3
	1.4	3.717 ± 0.002	36.5

Table 1: This table summarizes the angular frequency and χ^2/dof for every recorded undamped oscillation. The natural frequency varies based on the number of brass quadrants, but not amplitude, supporting the model proposed in Eq. 6.

Figure 3 plots natural angular frequency against the added moment of inertia due to brass quadrants. The resulting data is fitted to Eq. 7. The rotor's moment of inertia is measured as $I_0 = 6.65 \pm 0.046 \cdot 10^{-4}$ kg/m^2 fit with $\chi^2/\text{dof} = 0.120$. A $\chi^2/\text{dof} < 1$ indicates errors are overestimated for this fit.

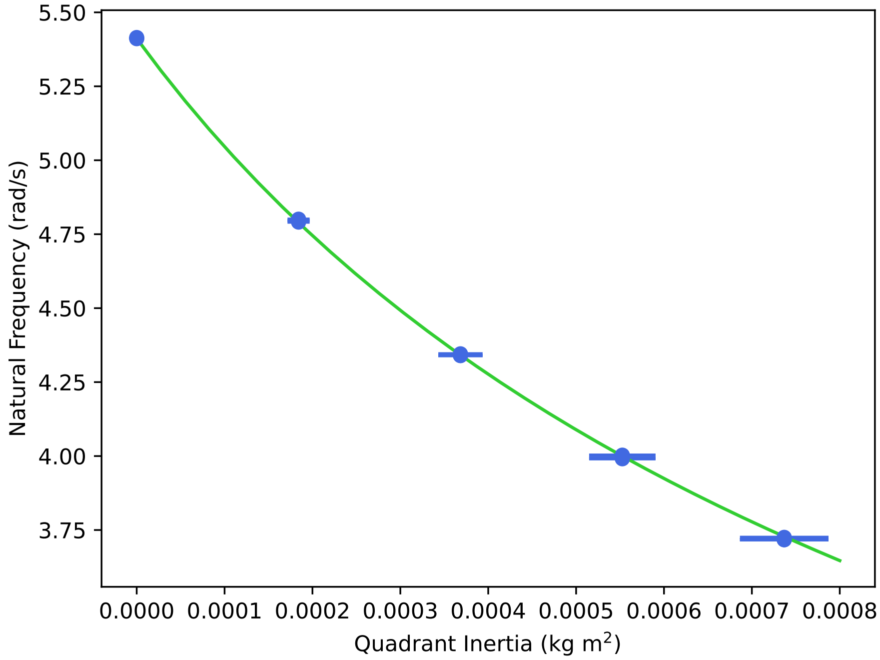

Figure 3: This plot displays the natural angular frequency of an undamped oscillator as a function of its moment of inertia. The resulting fit has $\chi^2/\text{dof} = 0.120$. Error bars are present, but small, for both axes.

Figure 4 plots angular displacement against time for a linearly damped and underdamped oscillator. The resulting data is fitted to Eq. 11. For this sample, $\gamma = 0.0757 \pm 0.0004\,\mathrm{kg\,m^2/s}$ and $\omega_0 = 5.4189 \pm 0.0004\,\mathrm{rad}$ with $\chi^2/\mathrm{dof} = 0.0009$. A $\chi^2/\mathrm{dof} < 1$ indicates the errors are overestimated for this sample. Despite this, the plot still visually models the behavior of the system well and produces a physically reasonable natural frequency.

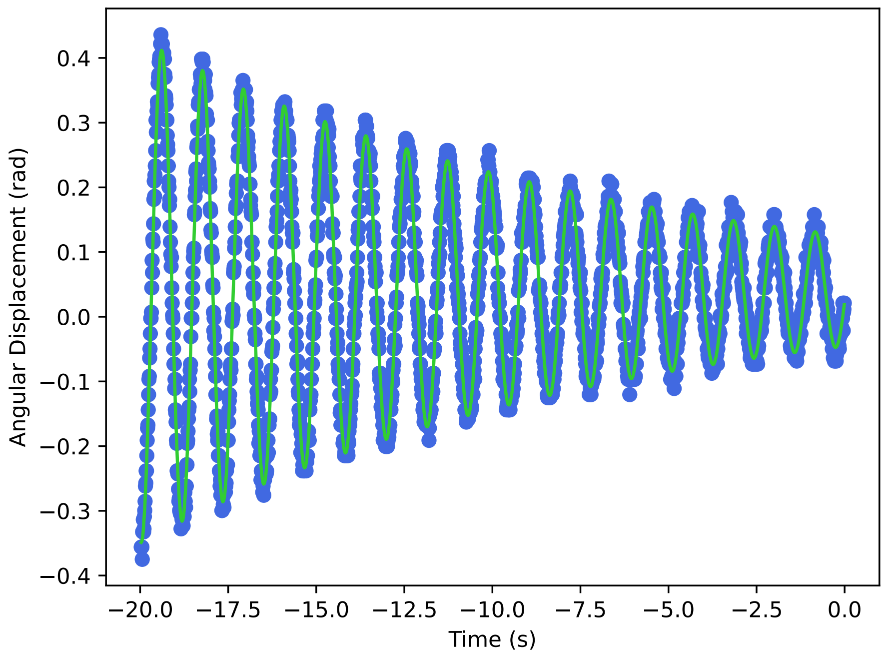

Figure 4: This plot displays the angular displacement of an linearly underdamped oscillator as a function of time. The resulting fit has $\chi^2/\mathrm{dof} = 0.0009$. Error bars are not included, as they obscure the data and fit when included.

Figure 5 plots angular displacement against time for a constantly damped oscillator. The resulting data is fitted to Eq. 17. This sample has $\omega_0 = 5.4061 \pm 0.0004\,\mathrm{rad}$ with $\chi^2/\mathrm{dof} = 0.966$. A $\chi^2/\mathrm{dof} \approx 1$ indicates the model fits the data accurately.

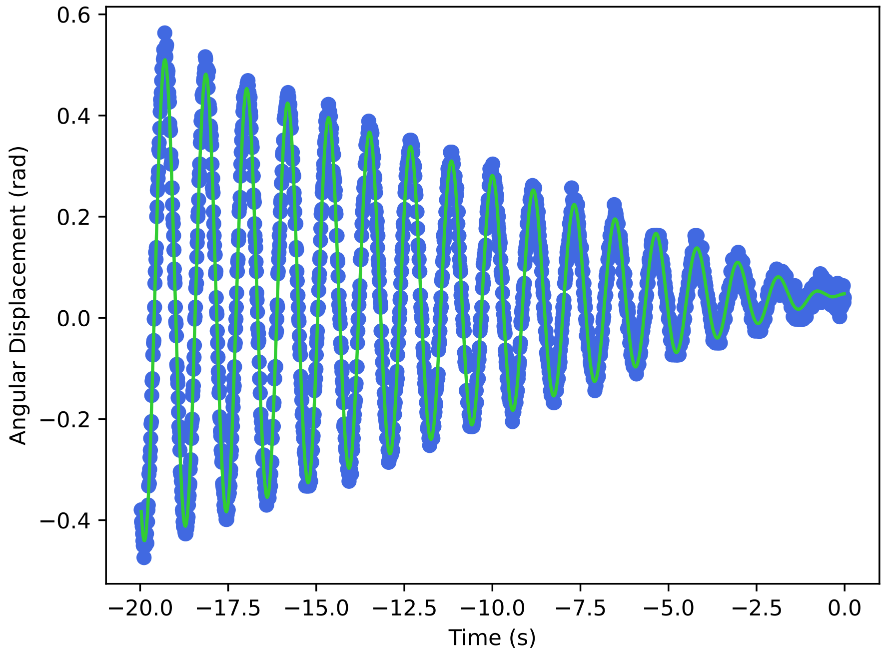

Figure 5: This plot displays the angular displacement of a constantly damped oscillator as a function of time. The resulting fit has $\chi^2/\mathrm{dof} = 0.966$. Error bars are not included, as they obscure the data and fit when included.

A Supplementary Information

A.1 Voltage to Angle Conversion

The angular position transducer on the torsional oscillator outputs a voltage related to the angular displacement of the rotor. This relationship is linear for small displacements, so the displacements in this experiment are all contained within this linear region. We can then convert between recorded voltages and the angular displacement of the rotor, given an oscilloscope waveform of voltages output by the transducer.

Figure 6 plots output voltage against visually recorded angular displacements of the torsional oscillator. These voltages were recorded using a digital multimeter with a precision of [2]

$$\sigma_V = 0.0015V + 0.001 \tag{18}$$

where V is the recorded voltage and σ_V is the uncertainty on that voltage.

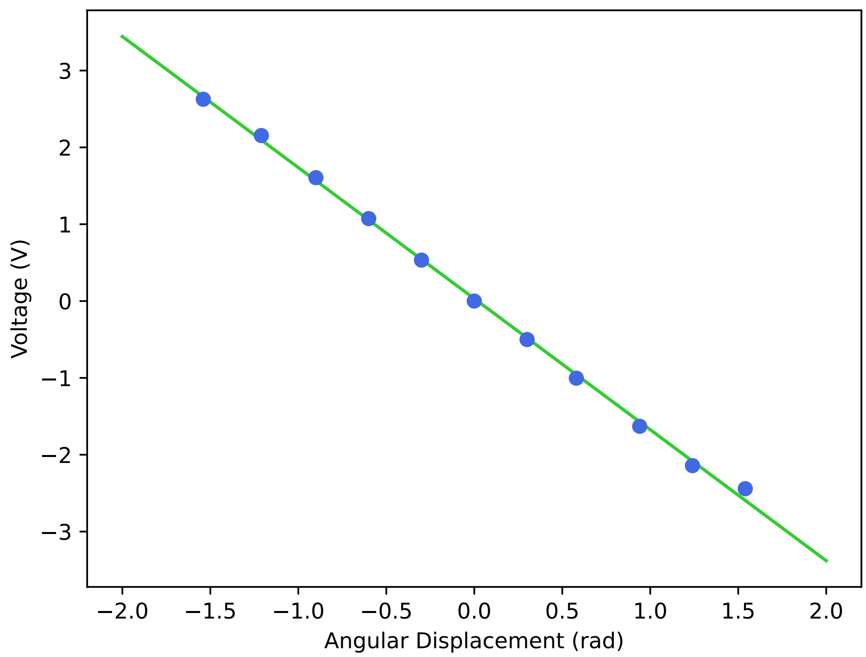

Figure 6: This plot displays the voltage output by the transducer as a function of angular displacement. The resulting fit has $\chi^2/\text{dof} = 11.5$ and is used to convert voltages to angular displacements throughout the lab. Error bars are present, but small, for both axes.

This data was fit to a linear function, which gives a slope $m = -1.705 \pm 0.021\,\text{V/rad}$ and y-intercept $b = 0.032 \pm 0.020\,\text{V}$ with $\chi^2/\text{dof} = 11.5$. A $\chi^2/\text{dof} > 1$ indicates errors are underestimated for this fit, but the value is close enough to 1 to be considered reliable for this experiment. The error σ_θ on angular displacements calculated with this conversion can be found as follows:

$$\sigma_\theta = \left(\frac{V-b}{m^2}\right)^2 \sigma_m^2 + \left(\frac{1}{m}\right)^2 \sigma_V^2 + \left(\frac{-1}{m}\right)^2 \sigma_b^2 \tag{19}$$

A.2 Undamped Oscillation Derivation

Consider the definition of angular momentum $\vec{L}$ for a point particle with nonzero mass and velocity:

$$\begin{aligned}\vec{L} &= \vec{r} \times m\vec{v} \\ &= \vec{r} \times \vec{p} \\ &= m\vec{r} \times \vec{v}_\perp \\ &= m\vec{r} \times (\vec{\omega} \times \vec{r})\end{aligned} \tag{20}$$

where:

- $\vec{L}$ is angular momentum
- $\vec{r}$ is the position vector
- m is mass
- $\vec{v}$ is velocity
- $\vec{v}_\perp$ is the component of velocity perpendicular to $\vec{r}$
- $\vec{\omega}$ is angular velocity
- $\vec{p}$ is linear momentum

A tensor-based expression of $\vec{L}$ can be derived by expanding the final expression listed in Eq. 20:

$$\vec{L} = \begin{bmatrix} y^2+z^2 & -xy & -zx \\ -xy & z^2+x^2 & -yz \\ -zx & -yz & x^2+y^2 \end{bmatrix} \begin{pmatrix} \omega_x \\ \omega_y \\ \omega_z \end{pmatrix} = \boldsymbol{I}\vec{\omega} \tag{21}$$

where:

- (x, y, z) are the Cartesian coordinates of the point particle
- $(\omega_x, \omega_y, \omega_z)$ are the Cartesian components of the point particle's angular velocity
- $\boldsymbol{I}$ is the moment of inertia tensor

This result will hold for a system of particles; each particle's contribution to the angular momentum can be summed to generate a net angular momentum. A solid object can then be modeled by integrating the above equation over the volumetric bounds of the solid, treating the point particles as infinitesimals of the object.

Torque $\vec{\tau}$ is defined as the derivative of $\vec{L}$:

$$\frac{d\vec{L}}{dt} = \vec{\tau} \tag{22}$$

$\boldsymbol{I}$ is constant with time, so $\vec{\tau}$ can be expressed as

$$\vec{\tau} = \boldsymbol{I}\frac{d\vec{\omega}}{dt} = \boldsymbol{I}\ddot{\vec{\theta}} \tag{23}$$

where $\ddot{\vec{\theta}}$ is the angular acceleration of the point particle.

Since the oscillator only rotates along a single axis, its motion can be modeled using the one-dimensional differential equation given in Eq. 3, where the vector $\ddot{\vec{\theta}}$ and tensor $\boldsymbol{I}$ are replaced with corresponding scalers.

A.3 Brass Quadrant Moment of Inertia

The brass quadrants used in this experiment have a mass of $213.6 \pm 0.2\,\mathrm{g}$. This value was determined by averaging the mass of all eight quadrants available for use with the apparatus. The quadrants are hollow circular quadrants with dimensions as follows, recorded using a ruler:

- Inner radius $r_i = 2.20 \pm 0.05\,\mathrm{cm}$
- Outer radius $r_o = 4.70 \pm 0.05\,\mathrm{cm}$
- Height $h = 1.90 \pm 0.05\,\mathrm{cm}$

The moment of inertia I of these quadrants and its uncertainty σ_I can be found using the following expressions:

$$I = \frac{m}{2}\left(r_o^2 - r_i^2\right) \tag{24}$$

$$\sigma_I = \sqrt{\left(\frac{\left(r_o^2 - r_i^2\right)}{2}\right)^2 \cdot \sigma_m^2 + \left(m r_o^2\right)^2 \cdot \sigma_{r_i}^2 + \left(m r_i^2\right)^2 \cdot \sigma_{r_o}^2} \tag{25}$$

These calculations give $I = 1.842 \pm 0.126 \cdot 10^{-4}\,\mathrm{kg\,m^2}$.

References

[1] TeachSpin, Inc. *Torsional Oscillator Preface, Chapters 0-2*, 2025.

[2] Fluke 170 series true-rms digital multimeters. `https://dam-assets.fluke.com/s3fs-public/6011663a-en-17x-ds-w_0.pdf?VersionId=e8AO6eNJpPsAUIhODD5LuxcacBfVJIy9`, 2025.